Temporal and spatial dynamics of CO_2 air-sea flux in the Gulf of Maine

D. Vandemark,[1] J. E. Salisbury,[1] C. W. Hunt,[1] S. M. Shellito,[1] J. D. Irish,[2] W. R. McGillis,[3] C. L. Sabine,[4] and S. M. Maenner[4]

Received 14 May 2010; revised 8 October 2010; accepted 15 October 2010; published 21 January 2011.

[1] Ocean surface layer carbon dioxide (CO_2) data collected in the Gulf of Maine from 2004 to 2008 are presented. Monthly shipboard observations are combined with additional higher-resolution CO_2 observations to characterize CO_2 fugacity (fCO_2) and CO_2 flux over hourly to interannual time scales. Observed fCO_2 and CO_2 flux dynamics are dominated by a seasonal cycle, with a large spring influx of CO_2 and a fall-to-winter efflux back to the atmosphere. The temporal results at inner, middle, and outer shelf locations are highly correlated, and observed spatial variability is generally small relative to the monthly to seasonal temporal changes. The averaged annual flux is in near balance and is a net source of carbon to the atmosphere over 5 years, with a value of +0.38 mol m^{-2} yr^{-1}. However, moderate interannual variation is also observed, where years 2005 and 2007 represent cases of regional source (+0.71) and sink (−0.11) anomalies. We use moored daily CO_2 measurements to quantify aliasing due to temporal undersampling, an important error budget term that is typically unresolved. The uncertainty of our derived annual flux measurement is ±0.26 mol m^{-2} yr^{-1} and is dominated by this aliasing term. Comparison of results to the neighboring Middle and South Atlantic Bight coastal shelf systems indicates that the Gulf of Maine exhibits a similar annual cycle and range of oceanic fCO_2 magnitude but differs in the seasonal phase. It also differs by enhanced fCO_2 controls by factors other than temperature-driven solubility, including biological drawdown, fall-to-winter vertical mixing, and river runoff.

Citation: Vandemark, D., J. E. Salisbury, C. W. Hunt, S. M. Shellito, J. D. Irish, W. R. McGillis, C. L. Sabine, and S. M. Maenner (2011), Temporal and spatial dynamics of CO_2 air-sea flux in the Gulf of Maine, *J. Geophys. Res.*, *116*, C01012, doi:10.1029/2010JC006408.

1. Introduction

[2] The exchange of CO_2 between the atmosphere and ocean is recognized as a key regulator, which buffers the contemporary rise of levels of this greenhouse gas in Earth's atmosphere. Many recent and ongoing observation and modeling investigations have focused on the precise estimation, monitoring, and prediction of this exchange in the open ocean [cf. *Takahashi et al.*, 2009; *Doney et al.*, 2009]. Developing these same capabilities for the coastal ocean represents an important topic of research because elevated rates of biologically mediated carbon cycling and land-ocean carbon input underscore the point that marginal shelf regions hold the greatest potential to significantly modify present and future global ocean CO_2 fluxes. One hurdle to clarifying the role of the coast within global air-sea flux budgets and models is the fact that the gas exchange and its controls typically exhibit larger magnitudes and are more dynamic in both space and time for coasts than for the open ocean. Field observations conducted in many marginal shelf areas are helping to address this issue and are now of the breadth where synthesis activities have been undertaken [e.g., *Cai et al.*, 2006; *Chen and Borges*, 2009; *Chavez and Takahashi*, 2007]. However, these works indicate that reported data are often subject to large uncertainties due to limited sampling, and that more long-term, high-resolution oceanic CO_2 observations are needed in coastal settings to assess uncertainty, to provide the data needed to confront models, and to characterize key controlling processes.

[3] The motivations for the present study are twofold. First, we wish to document the annual and seasonal cycle of CO_2 air-sea exchange in the Gulf of Maine, a marginal sea at temperate latitudes that is important to the North American coastal ocean carbon (C) budget, due to its extensive productivity and land-to-ocean C transport. The physical, biological, and chemical oceanography of this region has been

[1]OPAL, EOS, University of New Hampshire, Durham, New Hampshire, USA.
[2]Ocean Engineering Program, University of New Hampshire, Durham, New Hampshire, USA.
[3]Lamont-Doherty Earth Observatory at Columbia University, Palisades, New York, USA.
[4]NOAA Pacific Marine Environmental Laboratory, Seattle, Washington, USA.

0148-0227/11/2010JC006408

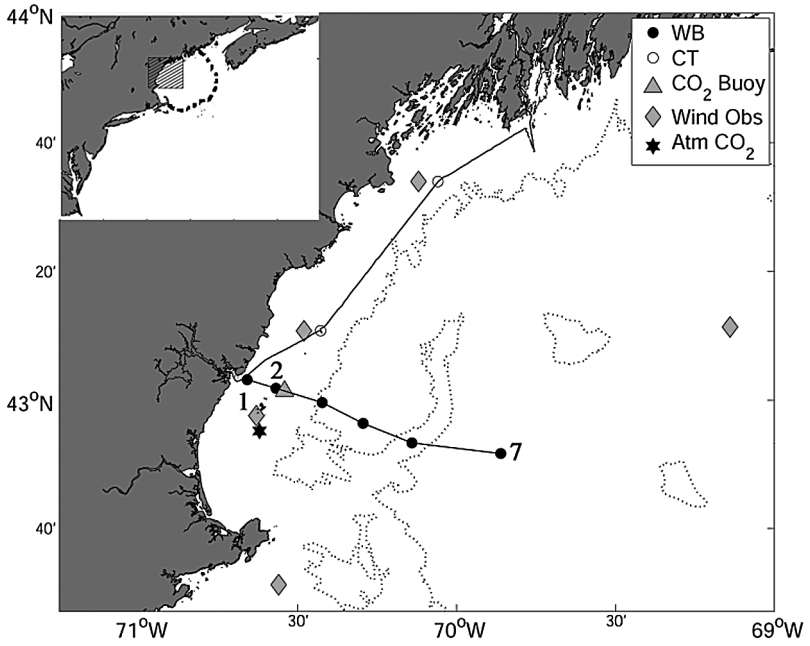

Figure 1. Map of the study region including the station locations for two UNH monthly shipboard measurement transects, the cross shore Wilkinson Basin (WB) and alongshore coastal (CT) transects, as well as a moored time series MAPCO2 buoy and a long-term atmospheric CO_2 observation site (Appledore Island at 70°40′W). Hourly meteorological data are available from the indicated wind observing nodes including NDBC IOSN3, 44005, and 44030. The CO_2 buoy is located at station WB2, while the farthest WB station to the east is WB7 located in the deep (>300 m) Wilkinson Basin. The inset shows the U.S. east coast down to Cape Hatteras NC in the south, our measurement region (crosshatch) and a dashed line bounding the seasonally stratified portion of the Gulf of Maine.

studied for decades [*Bigelow*, 1927; *Riley*, 1957; *Brooks*, 1985; *Townsend*, 1991], yet few measurements of inorganic C and surface water CO_2 exist [cf. *Chavez and Takahashi*, 2007; *Salisbury et al.*, 2009]. Seasonal stratification and high primary productivity rates in the Gulf of Maine [*O'Reilly and Busch*, 1984; *Balch et al.*, 2008] might imply that this region acts as an atmospheric C sink, yet the region's significant riverine C input, coupled with significant physical controls tied to temperature, tidal, and wind dynamics, leaves source versus sink status as an open issue. Clearly, an estimate of the air-sea CO_2 flux is a required, but unresolved, component in C budget closure for the Gulf of Maine and along the northern U.S. seaboard, augmenting recent efforts by *DeGrandpre et al.* [2002] and *Jiang et al.* [2008].

[4] Second, we wish to examine the magnitude of variability observed in space and time within the setting of this biophysically dynamic coastal ocean, particularly with respect to aqueous CO_2. There are logistical limitations in any observational effort and a key question in coastal biochemical studies is how much information is missing or in error when one neglects temporal or spatial under sampling. Two recent examples dealing with this question are found in the works of *Schiettecatte et al.* [2007] and *Jiang et al.* [2008]. To address this issue, one ideally needs to oversample in space and time and do this over a long time period to observe multiple realizations of key processes and time scales. Few field programs are able to accomplish such measurements [cf. *Friederich et al.*, 2002; *Bates*, 2001; *Keeling et al.*, 2004], and most are not in coastal waters.

[5] This paper presents observations from a multiyear time series study within the western Gulf of Maine with the dual objectives of (1) characterizing the air-sea CO_2 flux for this biome and (2) assessing this exchange and surface ocean CO_2 dynamics at space scales of 2–100 km and time scales from hours to years within the Gulf of Maine. To support our analyses, monthly shipboard flow-through data are combined with meteorological and CO_2 data taken hourly at a fixed station. We present measurements from repeat sampling for the period 2004–2008, evaluate and quantify measurement uncertainty associated with terms in the air-sea exchange equation, and then document and discuss the observationally informed CO_2 gas exchange results for this region. The study focus is primarily on this flux rather than the evaluation of the processes controlling oceanic CO_2, which are addressed elsewhere [*Salisbury et al.*, 2009] and will be studied in subsequent investigations.

2. Methods

2.1. Study Site

[6] The Gulf of Maine (GOM) is a marginal sea bounded by Cape Cod to the south and Nova Scotia to the east (Figure 1, inset). Physical characteristics include a large semidiurnal tide, a persistent counter clockwise gyre circulation with several distinct coastal currents [*Pettigrew et al.*, 2005], an uneven coastline and bathymetry with a predominately mud and gravel bottom, and large seasonal freshwater inflow [*Salisbury et al.*, 2008]. It is separated from the open

Atlantic by Georges and Browns Banks, and much of the seasonal to interannual circulation control is attributed to variations in shelf-sea exchange through the narrow Northeast Channel and fresher coastal source waters from along the Scotian shelf [e.g., *Townsend*, 1991; *Pringle*, 2006]. The region as a whole is well known for its high gross productivity [*Townsend et al.*, 2006] and extensive commercial fishing activities. The Western Gulf of Maine (WGOM), our study domain shown in Figure 1, lies within a seasonally-stratified portion of the GOM [*Pettigrew et al.*, 2005] where heat and buoyancy fluxes exceed tidal and wind-driven mixing forces from roughly March to November each year. This domain is also regularly impacted by local and distant river runoff from April to July of each year, with a resulting increase in buoyancy flux and coastal current velocities [*Geyer et al.*, 2004; *Salisbury et al.*, 2008] and decrease in surface water residence times [*Manning et al.*, 2009]. In general, coastal upwelling and downwelling length scales are O(10–20 km) and durations are 2–4 days. For the sake of comparison with other studies and regional C budgets, we assume that our study site is representative of the seasonally stratified Gulf of Maine [*Bisagni*, 2003], an area of roughly 10^5 km^2, comprising 55% of the GOM (see dashed line on Figure 1, inset). The surface area associated with inner (0–20 m), middle (20–50 m), and outer (>50 m) shelf depths within this domain are computed from USGS survey data as 5.7%, 8.9%, and 85.4%, respectively. This portion of the GOM thus represents a deeper bathymetric profile than for the shallower and sloping NW Atlantic shelves to the south [*DeGrandpre et al.*, 2002; *Jiang et al.*, 2008].

2.2. Methods and Materials

[7] A monthly shipboard Western GOM measurement program was initiated in 2004 to develop baseline data supporting improved ecosystem description and monitoring. Ocean surface layer CO_2 was measured from 2004 to 2008 as part of this program. The R/V Gulf Challenger was used to collect data on the two single-day transects shown in Figure 1. The primary (*ca*) monthly line runs across shore, roughly 80 km west to east, and ends at Wilkinson Basin (WB). The secondary Coastal Transect (CT) was taken seasonally alongshore north to the large Kennebec-Androscoggin river estuary. Discrete water samples and vertical profiler measurements were routinely taken at stations along these transects as marked in Figure 1. The cross-shore WB line is the focus of this study, in part because an array of nearby oceanic and meteorological observations is available to support this and other studies. As noted in Figure 1, the second WB station (WB2) from the coast lies roughly along the 50 m isobath and less than 15 km from two long-term buoys (GoMOOS 44030 and UNH CO_2), a long-term NDBC meteorological station (IOSN3), and the UNH AIRMAP atmospheric trace gas measurement tower on Appledore Island. Station WB2 is within 2 km of the UNH CO_2 buoy, and data from these two sites are combined in this study. For comparison with previous shelf studies we have divided the WB line data into inner, middle, and outer shelf sections. Only the innermost station (WB1) at 20 m can match the typical inner shelf definition as the depth reaches 50 m just 5 km from the coast. The composite data set used here includes 59 WB and 26 CT cruises.

[8] Measurements of CO_2 and other ancillary parameters needed to address the air-sea flux have been assembled from several sources. A monthly time series of sea surface (water intake at 0.7 m) temperature and salinity (Seabird SBE45), atmospheric pressure (Vaisala), and surface water and atmospheric CO_2 molar fraction (xCO_2) were all measured by a continuously operated shipboard flow-through system, with data recorded at 1 Hz and then postprocessed to 20 s sample output. For oceanic xCO_2, the water was pumped to an equilibrator, similar to that described by *Wanninkhof and Thoning* [1993], but consisting of three Plexiglas chambers instead of a single chamber. Measured differences between intake and equilibrator water temperature were negligible, as were pressure differences between ambient and equilibrator pressures. Equilibrated air was drawn out of the third chamber, while ambient air was drawn into the first chamber and passed through the second and third chambers, equilibrating with the pumped water supply at each step. Equilibrated air was drawn at 100 mL/min through tubing containing a Nafion selectively permeable membrane (Perma Pure, Toms River, NJ) with a counterflowing stream of dry nitrogen to remove water vapor from the sample gas stream. After drying, the sample was pumped to a nondispersive infrared gas analyzer (Li-cor, LI-6262, or LI-840) to measure the xCO_2 of the sample stream. The analyzer was calibrated several times per day with pure nitrogen (0 ppm xCO_2) and a gas mixture of 832 ppm CO_2 (Scott-Marin, Riverside, CA). Correction of all study CO_2 data for water vapor pressure and sea surface temperature and conversion between xCO_2 and the fugacity of carbon dioxide (fCO_2) were carried out according to standard methods [*Dickson et al.*, 2007]. Atmospheric xCO_2 was either periodically (2004–2005) or continuously (2006 to present) measured while the ship was underway. Ambient air was drawn from the ship's bow through a length of Teflon tubing, dried, and pumped into an NDIR analyzer as described above. Precision of resulting fCO_2 measurements is estimated at ± 3 μAtm.

[9] The UNH CO_2 buoy near station WB2 provides data recorded onboard a 1.9 m discus buoy moored 7 km northeast of the Appledore Island tower and 12 km offshore (43.01°N, 70.55°W). Water depth at the buoy is 65 m. Operation of the buoy's autonomous CO_2 data collection system (MAPCO2) is a joint collaboration between UNH and NOAA's Pacific Marine Environmental Laboratory. Buoy measurements of atmospheric and surface layer oceanic xCO_2 are collected every 2 h (2006) or 3 h (2007 to present) using an automated equilibrator-based gas collection system and an NDIR gas analyzer (Li-820, Li-Cor) based on the approach of *Friederich et al.* [1995]. The height of the atmospheric intake is 1.5 m above sea level (asl), and the depth of the water intake is 0.6 m. Calibration is performed immediately prior to these measurements using a soda lime ($CaCO_3$) reservoir for zero CO_2 reference and xCO_2 span tank (500 ppm) calibrated with standards at NOAA/ESRL. Field validations indicate the accuracy of this CO_2 measurement system is better than 3 ppmv [*Shellito et al.*, 2008].

[10] Continuous fast rate xCO2 measurements are available for several extended time periods between 2004 and 2008 from atop the AIRMAP tower 36 m asl on Appledore Island. Data are collected at 1 Hz and averaged to 0.5 h periods. Ambient air is drawn from a 5.1 cm i.d. Teflon manifold into an NDIR analyzer (Li-7000, Li-Cor). The analyzer is

automatically zeroed with ultrahigh purity nitrogen every 12 h and calibrated every 14 h with a range of standards (Scott-Marrin, Inc., Riverside, CA). Calibration standards range between 370 and 400 ppmv ± 1% and are used in the system for approximately 1 year. Agreement between the buoy MAPCO2 atmospheric xCO_2 data, and this AIRMAP station is observed to be ±1.7 ppmv [*Shellito et al.*, 2008].

[11] Continuous hourly wind speed and sea state measurements for 2004–2008 are produced from a composite of the surrounding meteorological stations available near the WB line. The primary source of wind speed data is buoy, ISON3, located near Appledore Island, for the inner and middle shore segments. For the offshore end of the WB line data, we use buoy N44005, located NE of WB7 (see Figure 1). Two wind values are used because we find a slightly elevated wind speed offshore (on average +0.5 m/s). However, we note that the linear correlation coefficient between five long-term meteorological stations across the region (IOSN3, 44029, 44030, 44007, 44009, and 44005) exceeds an R^2 of 0.95, affirming that winds are nearly uniform over our roughly 150 by 150 km measurement domain. All wind speeds are converted from the observed value to a neutral stability wind speed at 10 m asl using the Toga-Coare 3.0 bulk flux algorithm [*Fairall et al.*, 2003] including use of hourly water and air temperature, pressure, and relative humidity measurements.

2.3. Air-Sea Fluxes and CO_2 Disequilibrium Computations

[12] All air-sea CO_2 flux (F) values are estimated using a commonly employed parameterization based on a gas transfer velocity (k) and the disequilibrium between dissolved CO_2 gas concentrations, $[CO_2]$, across the surficial air-sea boundary layer. Formulations are given as

$$F\left(\mathrm{mol\,m^{-2}h^{-1}}\right) = \mathrm{k_{6xx}}(Sc/6\mathrm{xx})^{-0.5}\left([\mathrm{CO_2}]_{\mathrm{aq}} - [\mathrm{CO_2}]_{\mathrm{atm}}\right) = k_{\mathrm{w}}K_0\left(f\mathrm{CO_{2aq}} - f\mathrm{CO_{2atm}}\right), \quad (1)$$

where K_0 is the aqueous (aq) phase gas solubility given as function of salinity and temperature [*Weiss*, 1974], atmospheric CO_2 carries the (atm) subscript, *Sc* is the Schmidt number [*Wanninkhof*, 1992], and gas transfer velocity subscripts 6xx and w refer to wind-related models produced in the literature at values of 600 or 660. Following the work of *Jiang et al.* [2008], we produce hourly estimates for k_{w} (and F) using five candidate k_{6xx} algorithms [*Wanninkhof*, 1992; *Nightingale et al.*, 2000; *Wanninkhof and McGillis*, 1999; *McGillis et al.*, 2004; *Ho et al.*, 2006]. All models are formulated with a quadratic or cubic dependence and implemented with the buoy-derived 10 m neutral stability wind speed.

3. Results

3.1. Time Series Observations

[13] Monthly and hourly measurements at station WB2 for the 5 year period from 2004 to 2008 are shown in Figure 2 to provide an overall view of temporal dynamics for the parameters involved in regional CO_2 air-sea flux computations. Similar variation in all observations is found across the measurement transects shown in Figure 1.

[14] Seasonal change in the hydrographic cycle can be observed in Figure 2c where sea surface temperature (SST) values range from 3 to 5°C in late March to 18–20°C in late August. Surface salinity in this region is quite fresh, with a mean value near 31.4 psu, and also variable at the monthly scale. For comparison, the GOM as a whole has a mean salinity near 32.3 psu, and the adjoining NW Atlantic shelf break is roughly 33.5 psu. Values during the spring period of April–June, when river flow is typically high due to snowmelt and rainfall, often drop to 28–29 psu at stations WB1–WB3. Both the SST and SSS curves represent a linear interpolation between monthly samples obtained within 5 km of WB2 on the sampling dates indicated by symbols in Figure 2a. The water column here is seasonally stratified [e.g., *Bisagni*, 2003] and the approximate date of the spring mixed layer formation and fall breakdown can be determined by the intersection of the SST and SSS curves during these seasons.

[15] The wind speed and sea state data in Figure 2d represent the hourly wind speed (U) observations as well as weekly averaged U and SWH. A pattern of increased wind speed from November to April in each year coincides with winter cooling below roughly 10°C, mixed layer deepening (offshore), and destratification (inshore). The lowest wind speeds occur in middle-late summer, coincident with the warmest SST. The sea state data typically follow U closely at the weekly to monthly time scale, in part because the GOM typically receives only weak swell from the NW Atlantic, and thus, the sea state is characteristically wind-driven. Some cross-shore variation in SWH under strong W and NW winds may be expected, but for this multiyear study, we present only SWH data taken from station 44030 near WB2.

[16] Figure 2a provides monthly shipboard fCO_2 measurements, along with a trace indicating linear interpolation to hourly values as well as 2 or 3 hourly buoy data when available. A repeatable seasonal cycle is apparent, with a minimum of 200–250 μAtm seen in most spring periods and an annual maximum of 400–500 μAtm observed in late fall to early winter. Summertime values consistently reside near 400 μAtm. Typically, the fCO_2 measurements taken by the buoy at a finer time resolution do not deviate more than 10–20 μAtm from the ship-based fCO_2 measurements; however, there are notable periods with deviations exceeding 50 μAtm.

[17] Ship-based atmospheric fCO_2 measurements, also roughly once per month, are shown in Figure 2b on the same scale as the ocean data. In this case, we present the median measurement value for the entire daily cruise in an attempt to filter out observed variability. The trace in Figure 2b does not represent a linear interpolation but rather a time-varying fCO_2 model developed using the hourly buoy and AIRMAP station data near WB2, as shown in Figure 3. Recently, several authors [*Padin et al.*, 2007; *Perez et al.*, 2001; *Jiang et al.*, 2008] have shown that atmospheric boundary layer CO_2 in the coastal zone frequently exhibits 5–20 μAtm variability at diel to multiday time scales. The data compiled in Figure 3 indicate that near our site this magnitude can be even greater and is O(20–40 μAtm) throughout the summer. While not shown, the largest values occur early in the morning near 500–700 AM local time, which we attribute to a routinely occurring shallow nocturnal boundary layer [*Zhou et al.*, 2005]. Summertime afternoon values (when our ship measurements typically occur) fall below the daily average value due to terrestrial photosynthesis and advected continental air.

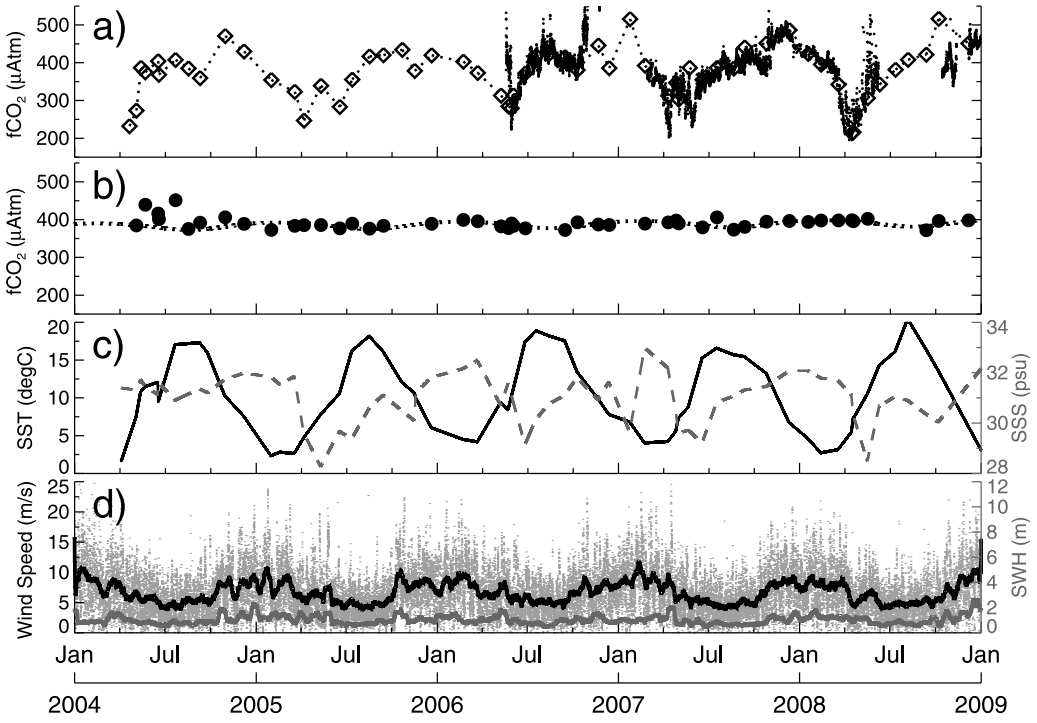

Figure 2. Multiyear observations of variables used to estimate CO_2 air-sea flux at station WB2: (a) the oceanic surface layer fCO_2 derived from monthly cruise measurements within 5 km of the station as well as bihourly mooring data (small symbols) collected by the UNH CO_2 buoy at WB2 (see Figure 1) and (b) the cruise median atmospheric fCO_2 (solid circle) along with a time-dependent model discussed in the text. (c) Monthly SST and SSS (dashed) shipboard data are linearly interpolated to hourly time step and (d) hourly 10 m wind speed as well as traces showing biweekly averaged significant wave height (lower trace) and wind speed (upper trace).

In the mean value and at a seasonal scale, Figure 3 indicates the local data significantly depart from the Mauna Loa atmospheric measurements often used as a Northern Hemisphere atmospheric reference in air-sea flux studies [e.g., *Bakker et al.*, 2001; *DeGrandpre et al.*, 2002; *McNeil et al.*, 2006; *Salisbury et al.*, 2008]. For this study, we choose to create an hourly estimate following the approach of *Padin et al.* [2007] where we develop a second-order harmonic fit to the observations in Figure 3 to produce a model covering the entire 2004–2008 period and given as

$$xCO_2(t) = a_0 + a_1\, t/\mathrm{dy} + a_2\, \sin((t - b_1)\phi) + a_3 \sin^2((t - b_2)\phi), \quad (2)$$

where $\phi = 2\pi/\mathrm{dy}$, dy is 365.25 (days of year), and a = [382, 2.1, −9.05, 1.10] and b = [138, −82]. Because observed atmospheric variations tend to be random about the weekly mean, the use of the model is considered a superior choice to linear interpolation [*Padin et al.*, 2007] of once per month ship-based values. For example, we find that monthly cruise data in Figure 3 sometimes fall 5–20 ppmv from this mean.

[18] Hourly CO_2 flux and ΔfCO_2 time series for the entire period are given in Figure 4, along with an annually repeating ΔfCO_2 climatology that we produce using an average over the 5 year period. Note that for any further 5 year averages involving ship data (not wind speed or k_w) the average is produced using data from days 107 to 365. Our time series began on day 107 in 2004 and thus days 1–107 represent a 4 year average. The seasonal cycle of ocean surface CO_2 seen in Figure 2 is reflected in Figure 4a with apparent spring ΔfCO_2 drawdown occurring between days 100 and 200. The CO_2 hourly flux time series in Figure 4b shows a strong qualitative correspondence with the seasonal ΔfCO_2 cycle,

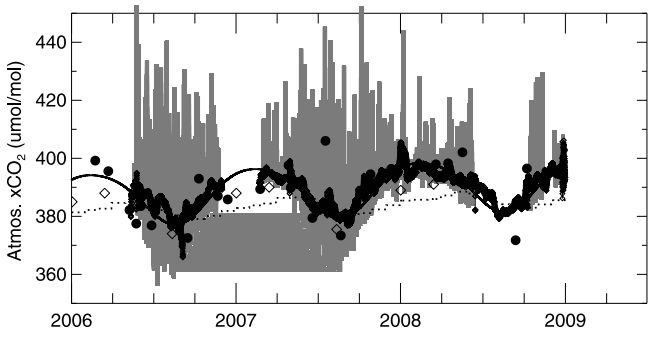

Figure 3. Data from the AIRMAP Appledore Island (30 min) site or the UNH CO_2 buoy (bihourly) are given over a multiyear period along with shipboard daily median samples (solid circle) and flask sample data from Sable Island Nova Scotia (diamond). The thicker solid trace is weekly averaged xCO_2 from the hourly stations. The vertical gray bars represent weekly minima and maxima in the hourly estimates. Also shown is the time varying xCO_2 model fit to the multiyear hourly data set (thin solid) and the monthly observations from Mauna Loa Hawaii station data (dashed trace).

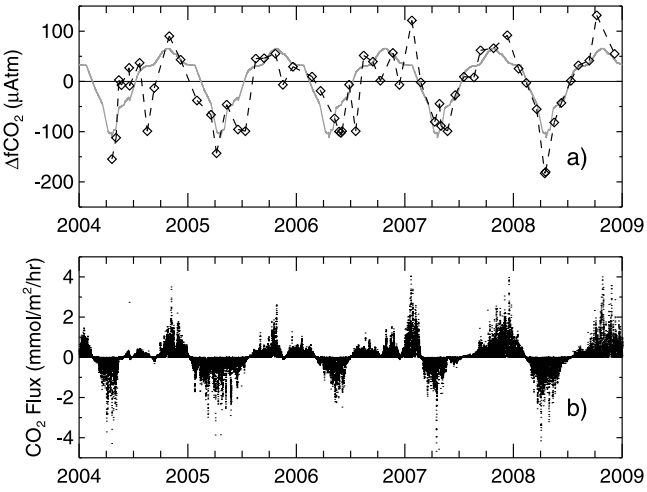

Figure 4. (a) Time series of observed sea-air CO_2 difference (symbols) and hourly interpolated data (dashed) at station WB2 as well as a repeating annual climatology (solid) produced from the 2004–2008 average at WB2. (b) The hourly flux is produced for the same period using hourly NDBC wind data and the gas transfer model of *Wanninkhof* [1992]. Note that days 001–107 fluxes in 2004 are produced using the ΔfCO_2 climatology rather than observations.

as is somewhat expected from the equation (1). Hourly flux measurements indicate significant minima and maxima associated with high-wind events following the chosen k_w algorithm [*Wanninkhof*, 1992], with the flux magnitude exceeding 4 mmol $m^{-2} h^{-1}$ on numerous occasions. Year-to-year variability is observed in both panels, with ΔfCO_2 data at times deviating from the climatology by values greater than 100 μAtm. Interannual differences in the extent and magnitude of spring influx and fall to winter efflux periods are seen in the flux time series.

[19] A monthly view of the annual air-sea flux cycle at WB2 is given in Figure 5 along corresponding controls, ΔfCO_2 and k_w. Data for the full period average, as well as the individual years 2005 and 2007, are shown to document both the mean seasonal cycle as well as years that deviate most strongly from this mean. The thickest traces in each panel provide the climatologies and seasonal cycles already seen in Figures 2 and 4. It is now apparent that ΔfCO_2 and the flux are effectively in phase. The periods with highest gas transfer velocity coincide with the positive ΔfCO_2 periods and thus accentuate the source of CO_2 to the atmosphere in the late fall to winter. The two individual years (2005 and 2007) generally follow the longer-term average, but there are also substantial monthly differences, especially during late fall and into winter. Estimates of the measurement standard deviation, computed over each monthlong period, are provided as a

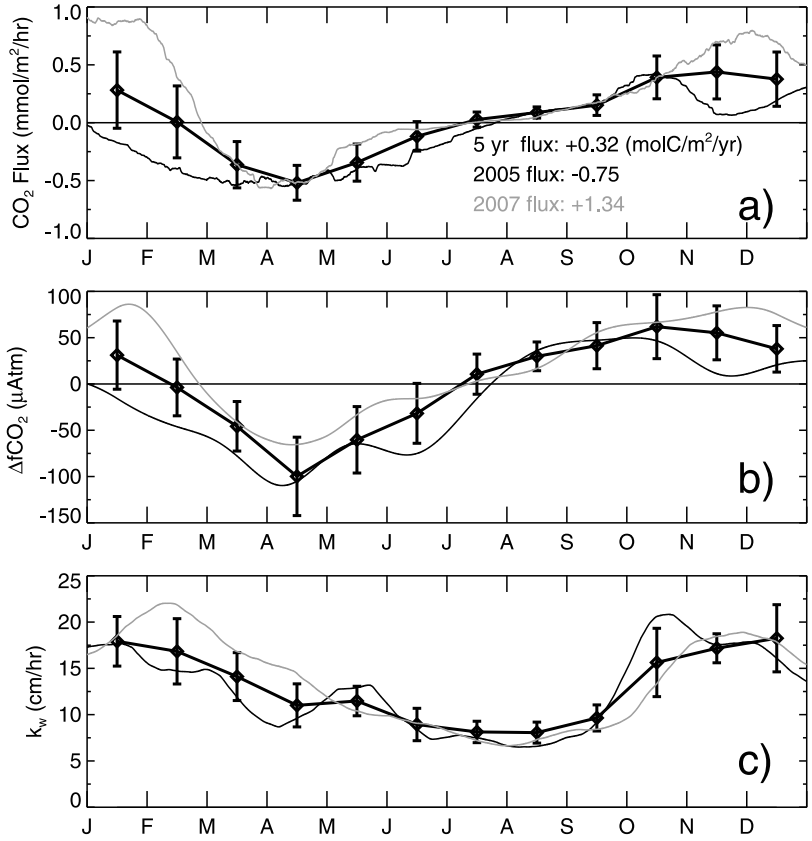

Figure 5. Monthly averaged estimates of (a) CO_2 flux, (b) ΔfCO_2, and (c) transfer velocity at WB2. Data show years 2005 (dark) and 2007 (light gray), depicted from a moving 30 day average over the hourly data, as well as the 5 year average (thickest trace). Error bars are one standard deviation over the monthly averaged results for the 5 year period and provide one measure of interannual dynamics in each month. Net annual flux values are provided in Figure 5a.

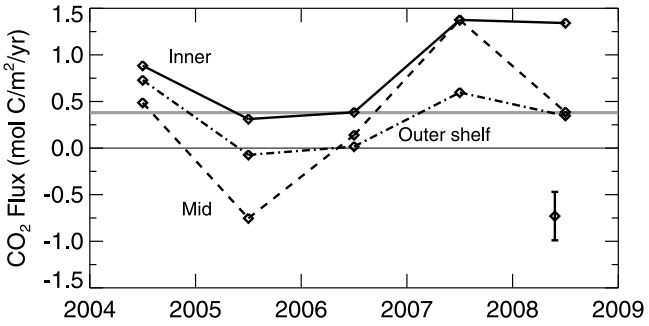

Figure 6. Net annual CO_2 flux for inner (solid), middle (dashed), and outer shelf (dash-dotted) sections of the Wilkinson Basin transect line. At the bottom right is the annual estimate uncertainty as discussed in the text. The straight gray line for the entire period at $F = 0.38$ mol m^{-2} yr^{-1} represents the region-wide 5 year average flux.

measure of year-to-year variation. Smallest error bars coincide with summer months and the lowest ΔfCO_2 and k_w. While the 5 year net annual flux (Figure 5a) shows station WB2 to be a net CO_2 source of +0.32 mol m^{-2} yr^{-1}, years 2005 and 2007 differ from this value by a significant amount, with year 2005 being a relatively strong sink (i.e., negative flux).

[20] The net annual flux in each year, and for different cross-shelf subsections, is shown in Figure 6 with values provided in Table 1. In all but three instances, the data indicate a positive flux (export of CO_2 to the atmosphere). Year 2006 appears to be in net balance region wide, while year 2005 is the anomalous case indicating a sink on the inner and middle shelf regions. Similar year-to-year variation for all stations indicates the three shelf subregions generally agree with each other at an annual scale to better than ±0.5 mol m^{-2} yr^{-1}. The inner shelf does consistently exhibit the largest positive flux values. The estimated uncertainty for these annual averages is ±0.26 mol m^{-2} yr^{-1} and is shown on Figure 6 in the lower right corner.

3.2. Spatial Variability

[21] The net annual flux values shown in Figure 6 also provide a first measure of the spatial variability observed cross shore on the WB monthly transects. As shown in Figure 1, the data collection extends from shore to roughly 80 km east into the GOM at Wilkinson Basin, where depths exceed 300 m. We produce flux estimates for inner (0–50 m depth), middle (50–100 m), and outer (>100 m) shelf segments of the WB line following methodologies from previous marginal shelf air-sea flux studies [*DeGrandpre et al.*, 2002; *Jiang et al.*, 2008]. Note that the bottom in the GOM drops off quickly (>60 m at 10 km from shore) and does not slope smoothly along the WB line, and thus, our segments and locale are not ideal representations of this type of division. For this study, we assume the wind speed (and k_w) are spatially uniform over the roughly 100 km^2 region. Therefore, most spatial variation in the computed flux comes from variation in ΔfCO_2, with a change due to SST and salinity small enough to be negligible. Therefore, the oceanic fCO_2 data are used as a surrogate for describing observed spatial flux variability on a given day.

Table 1. Annual and Multiyear Sea-Air CO_2 Flux Estimates for the Study Region[a]

	2004	2005	2006	2007	2008	5 Year
Inner	0.91	0.31	0.38	1.37	1.07	0.81
Middle	0.51	−0.75	0.14	1.34	0.35	0.32
Outer	0.75	−0.15	0.02	0.60	0.47	0.35
Region[b]	0.74/0.68	−0.11/−0.10	0.05/0.05	0.71/0.65	0.49/0.46	0.38/0.35

[a]With units mol m^{-2} yr^{-1} and with positive values being a source to the atmosphere. Estimates for the inner, middle, and outer shelf as well as a weighted average representing the seasonally stratified Gulf of Maine are provided.

[b]The second values are derived from an ensemble average of fluxes separately estimated using the five k_w algorithms discussed in section 2. All other values utilize *Wanninkhof* [1992].

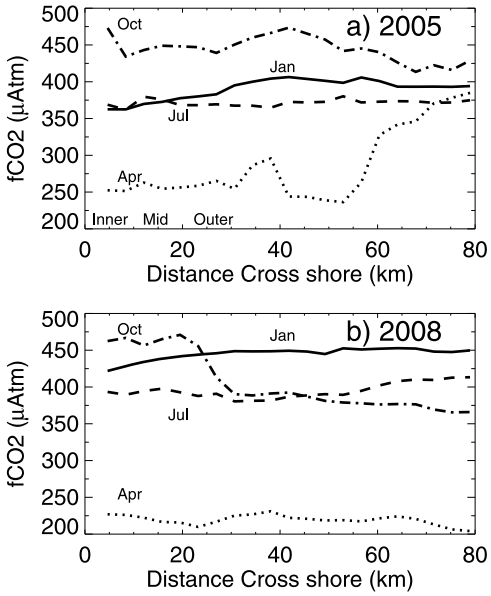

Figure 7. Example daily shipboard WB transect fCO_2 measurements averaged (3 km smoothing) over cross shore legs with the month of each cruise noted for (a) year 2005 and (b) year 2008. The deepwater Wilkinson Basin station lies at 80 km, while the inner and middle shelf stations fall at 0–8 and 8–15 km, respectively.

[22] Cross-shore variation of daily fCO_2 for several months and in two different years is presented in Figure 7. The traces represent a 2 km along-track smoothing of shipboard flow-through data, averaged at 20 s intervals, that typically has resolution below 100 m. January and July data indicate that fCO_2 varies less than 25 μAtm across the entire 80 km transect, with a smoothly varying change at the 40–80 km length scale. Similar behavior is seen for April 2008 and October 2005 transects. The two most variable transects show a 115 μAtm increase on the inner shelf in October 2008 and a 140 μAtm increase on the outer shelf for April 2005. These two largest values are still a factor of 2 lower than the seasonal pCO_2 signal observed from April to October. Overall, the data typically show variations of less than 5 μAtm occurring at spatial scales shorter than 10 km.

[23] A multiyear average of monthly fCO_2 for the inner, middle, and outer shelf segments is given in Figure 8. As in Figure 6 and Table 1, the three estimates agree to better than 20 μAtm in most months and present very similar seasonal

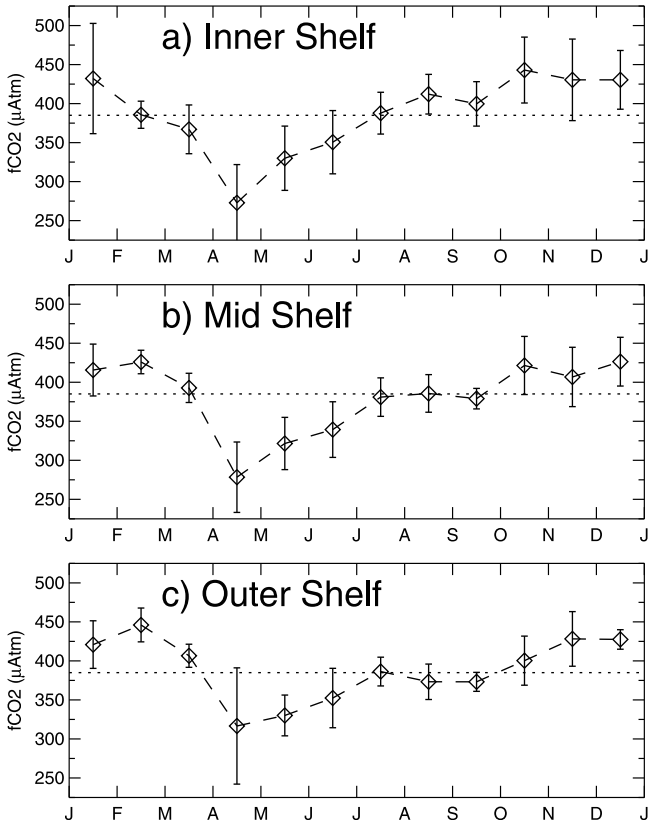

Figure 8. The 5 year average of surface layer fCO_2 for the (a) inner, (b) middle, and (c) outer shelf stations along the monthly WB transect. Vertical bars indicate ±1 standard deviation over all visits to each location in the given month (typically 5).

cycles. One indicator of interannual variability for each month and segment is provided using the standard deviation calculated over all years, which shows a similar level of variation at the three locations.

[24] Observed alongshore fCO_2 variation, measured along roughly the 50–60 m isobath on seasonal CT transects (see Figure 1), is presented in Figure 9. The middle 40–50 km of this transect is farther from the coast and river plumes, and in this transect segment, we see variation below 20–40 μAtm on most days. Data nearer the 0–10 and 60–80 km ends of the legs represent areas near the Piscataqua and Kennebec estuary outflows where more variability is expected due to salinity, temperature, and carbon dynamics [*Salisbury et al.*, 2009]. Only in April 2007 does one observe a strong alongshore fCO_2 gradient with a magnitude of 120 μAtm and lowest values in the south toward the WB transect line. This is not uncommon in the April–May period when local riverine input is greatest.

3.3. Air-Sea Flux Estimate Uncertainties

[25] It is difficult to accurately quantify the level of uncertainty to apply to monthly and annual air-sea flux estimates for a site or region, especially in coastal waters. While the ΔfCO_2 measurement accuracy may be high, one does not have complete coverage in either space or time. Nor is there a definitive method or parameterization for the gas transfer velocity [*Wanninkhof et al.*, 2009]. Here the error estimation conventions applied in numerous coastal studies are taken into account [e.g., *DeGrandpre et al.*, 2002; *Friederich et al.*, 2002; *Schiettecatte et al.*, 2007; *Kuss et al.*, 2006], with a particular emphasis given to the approach of *Jiang et al.* [2008]. We take a similar root mean square uncertainly approach to pose the potential error for a given monthly flux estimate as

$$\varepsilon F_{CO_2} = F\sqrt{\left[{\varepsilon_{kw}}^2 + {\varepsilon_{fCO_{2atm}}}^2 + {\varepsilon_{fCO_{2aqeous}}}^2\right]}, \qquad (3)$$

where ε is the relative standard error associated with k_w, the Weiss solubility assumption is assumed negligible in equation (1), and the latter two terms reflect measurement and sampling uncertainties (including relative error due to space and time interpolation) in the hourly air and sea fCO_2 values used to produce the fluxes. These error terms are assumed to be uncorrelated. As in the work of *Jiang et al.* [2008] and other works [e.g., *Wanninkhof et al.*, 2009; *Olsen et al.*, 2005], the relative error of the gas transfer velocity is taken to be 12%, including potential random error in the wind measurements. Following *Jiang et al.* [2008], we evaluated the flux obtained using the five algorithms listed in section 2 at flux averaging periods of hours to years. The differences amongst flux estimates are typically below 10% at the monthly scale and less than 3% at the annual scale, consistent with that observed in Table 2 of their study. As one attempt to summarize the impact and difference between choice of

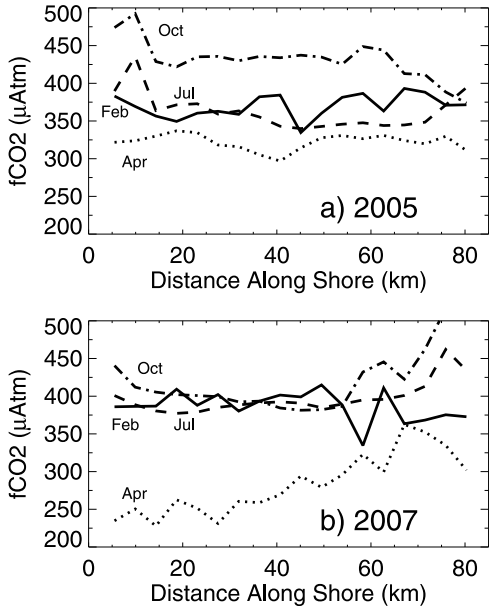

Figure 9. Example of daily shipboard data from alongshore coastal transect fCO_2 measurements averaged (3 km smoothing) over the south to north sampling track shown in Figure 1. The month of each cruise is noted for (a) year 2005 and (b) year 2007. Distances of 20–70 km on this leg run along the 50 m isobath, while the mouth of the Kennebec-Androscoggin rivers lies just north of the 80 km mark. Station CT1 (also NDBC 44030 and GoMOOS buoy B) lies near 43.2°N on Figure 1 at the 20 km alongshore distance.

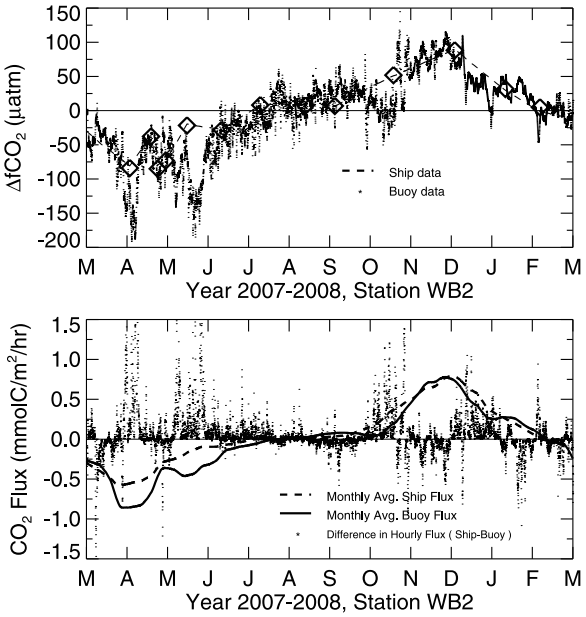

Figure 10. One year of ship and buoy-derived observations of (top) ΔfCO_2 and (bottom) CO_2 sea-to-air flux derived from hourly data sets at station WB2. Buoy ΔfCO_2 observations are at a 3 h time step, while the monthly ship measurement times are indicated by large symbols on the top. The difference between fluxes is shown at hourly time step (Figure 10, bottom) along with monthly smoothed flux estimates as indicated.

gas transfer model, the bottom row in Table 1 provides the regional annual fluxes obtained using our chosen standard gas transfer algorithm [*Wanninkhof*, 1992] and that obtained using the ensemble of the five algorithms. The difference is at the second digit in the annual values. The atmospheric CO_2 data of Figure 3, sampled at high temporal resolution, illustrate that observed deviations from our hourly xCO_{2atm} model estimates of equation (2) may often be significantly larger than the *Jiang et al.* [2008] atmospheric error estimate of ±6 μAtm estimated for the South Atlantic Bight. However, the computed monthly deviation between equation (2) and buoy-measured values over 20 months at buoy station WB2 yield a maximum error of 4 μAtm and a monthly standard error of 2 μAtm. We make the assumption that spatial variation impacts at a monthly scale are of this order. Combining these findings with a ±3 μAtm atmospheric CO_2 measurement error, we conservatively prescribe 3% for the second error term above.

[26] For coastal sites in particular, error due to undersampling the aqueous fCO_2 in a monthly or seasonal measurement program is a certain and potentially large source of error in flux calculations. As in most studies, the fCO_2 interpolation of monthly data used for Figure 4 and Table 1 assumes well-predicted behavior between ship measurement visits. However, most studies must either neglect an estimate of error due to this assumption or develop an ad hoc accounting because no data exist to resolve the issue. In this study, monthly shipboard data collection next to the mooring at WB2 permits sampling error assessment at one location. As part of this approach, we assume that the limited spatial variability in fCO_2 observed at 5–10 km length scales (see Figures 6 and 8) indicates that temporal dynamics dominate the error term $\varepsilon fCO_{2aqeous}$ in equation (3). A yearlong comparison of the ship and mooring-based estimates of fCO_2 and the derived flux at site WB2 is shown in Figure 10. The hourly wind (and k_w) data used to estimate the flux were identical, and thus, all differences come from ΔfCO_2. The results indicate hourly flux differences can be very large, at times exceeding the monthly mean values. Mooring data in the spring of 2007 show that [*ca*] monthly ship sampling missed significant CO_2 drawdown events at the 5–15 daytime scale. As a result, 25%–50% errors in the monthly fluxes are observed in April and May. On average, over a 22 month ship and buoy data evaluation at WB2, we find the monthly fCO_2 error due to temporal sampling is 16%. This factor will dominate $\varepsilon fCO_{2aqeous}$ and equation (3). Applying the overall rms error estimation model to monthly data sets for 2004–2008 yields an average monthly flux uncertainty of ±0.43 mol m^{-2} yr^{-1}. This monthly number is similar to that obtained by *Jiang et al.* [2008] for the SAB.

[27] If one assumes successive monthly sampling errors are independent and uses the central limit theorem to derive the annual and five-year uncertainty, then standard error (SE = standard deviation/$\sqrt{N}$) estimates become ±0.12 and ±0.05 mol m^{-2} yr^{-1}, respectively. However, the flux differences shown in Figure 10, especially in spring, indicate the potential for substantial systematic error over an annual period, at least in 2007–2008. For that period the mooring-derived net annual flux is +0.01 mol m^{-2} yr^{-1} while the ship-derived value is 0.43 mol m^{-2} yr^{-1}. This annual difference is of the order of our monthly standard error and significantly outside ±0.12 mol m^{-2} yr^{-1}. Thus, it is likely that monthly samples in the time series are not independent. One measure of this is seen in the computed temporal decorrelation (*e*-folding) time scale for the ocean fCO_2 buoy data at WB2. This time scale is roughly 45 days (a similar result is obtained using an autocorrelation evaluation of either hourly buoy data over 22 months or the 60 month monthly time series). Thus, there is a need to obtain an effective number of independent samples N'. N' can be derived from the actual sample number N and the lag-1 or first-order autocorrelation value (ρ) as suggested by *World Meteorological Organization* [1966] with $N' = N\,(1 - \rho)/(1 + \rho)$. In our case, the 1 month lag $\rho = 0.55$, $N' = 3$, and the average annual uncertainty for our study becomes ±0.26 mol m^{-2} yr^{-1}. This is the uncertainty (SE) level for net annual fluxes in Table 1 and shown on Figure 6.

4. Discussion

[28] The first objective of this observational program is to provide the first regional air-sea CO_2 flux characterization. A second is to establish a long-term coastal ocean CO_2 time series with temporal and spatial sampling resolution sufficient to shed new light on potentially unresolved dynamics and processes. As with the open ocean time series projects such as HOTS, BATS, and Carioca, these coastal data can help inform state-of-the-art ocean measurement and modeling efforts, as well as to help answer a common question in coastal CO_2 studies: What are we missing? We address these issues with our data sets with the understanding that not all

complexity in the observations and controlling coastal processes, especially at finer space and time scales, are included.

4.1. CO_2 Air-Sea Flux Dynamics and Net Annual Values

[29] A first conclusion, drawn from inspection of spatial and temporal data in Figures 7 and 9, is that regional horizontal gradients in ocean fCO_2 (and CO_2 flux) are typically small relative to seasonal time scale fCO_2 variations. The data indicate that surface water fCO_2 spatial variability in both cross-shore and alongshore directions from the WB2 middle shelf site is O(10–20 μAtm) on most occasions, while the peak-to-peak seasonal range is 150–200 μAtm. The observed spatial scale of fCO_2 gradients is typically longer than 20 km, especially for the cross-shore measurements (Figure 7). Such a length scale agrees with recent Gulf of Maine investigations [e.g., *Balch et al.*, 2004] where the relative homogeneity is attributed to mixing by energetic tidal and wind stress forcing occurring at daily to weekly time scales. Table 1 does indicate a small but consistent efflux increase for the inner shelf (depth < 20 m), a tidally mixed zone of limited area that lies within 5–10 km from shore in the Gulf of Maine. The elevated near shore values are also consistent with results observed to our south [*Boehme et al.*, 1998; *DeGrandpre et al.*, 2002]. Otherwise, we observe middle and outer shelf annual flux estimates that are statistically equivalent (Table 1 and Figure 6), and that the monthly and seasonal fCO_2 observations for inner, middle, and outer cross-shelf locations are also in near agreement (Figure 8; see also Figure 4 in *Salisbury et al.* [2009]). These conclusions rely on the assumption that ocean fCO_2 dynamics reflect air-sea flux dynamics, since observed spatial variations in hourly winds (and hence k_w) are small. Moreover, the multiyear data of Figure 4 indicates that spatial variation in fCO_2 and flux data will be greater in the 30–45 day spring and fall periods, when the mixed layer is in transition [see also *Salisbury et al.*, 2009]. Overall, given the similarity between stations along the WB transect out to the deep Wilkinson Basin end point, we assume that time series results near the CO_2 buoy site (station WB2) in 60 m of water can be considered as reasonably representative of the seasonally stratified Gulf of Maine, an area that encompasses most of the Gulf with the largest exceptions being the Bay of Fundy and Georges Bank. A fuller validation of this last assumption awaits data from ongoing and future observational efforts.

[30] The multiyear time series results of Figures 1, 4 and 5 document fairly consistent annual patterns in flux, ΔfCO_2, wind speed (and gas transfer velocity), while Figures 5a and 5b demonstrate a high temporal correlation between the flux and ΔfCO_2 data. This is not unexpected given equation (1) and the data in Figures 5b and 5c. The 5 year average flux in Figure 5a indicates a near sinusoid where the Gulf of Maine generally spends half the year (February to July) removing CO_2 from the atmosphere and the other half (August to February) releasing it. As seen in Figures 1 and 5, the strongest winds and gas transfer velocities coincide with the months of ocean-to-atmosphere CO_2 release, and at the 5 year time scale, this factor helps tip the balance toward the overall +0.38 mol m^{-2} yr^{-1} flux value. As some confirmation, if one computes the fluxes using only the mean 2004–2008 wind speed (U = 6.7 ms^{-1}), the 5 year flux values in Table 1 shift downward by an average of 0.35 mol m^{-2} yr^{-1}. This implies that with steady winds and all other factors and feedbacks unchanged, the air-sea exchange would have been in net balance.

[31] Across the region and in an annual net sense, the area acted as a net source of +0.38 ± 0.2 mol m^{-2} yr^{-1} over the period 2004–2008. Our long-term program provides data (see Figures 5 and 6) illustrating that while 3 of 5 years effectively match this 5 year average (WB2 is +0.32 in Figure 5a), years 2005 and 2007 differed substantially, 2007 being a substantially larger source (WB2 is +1.34) and 2005 as a net CO_2 sink (WB2 is −0.75). Thus, collecting data in only 1 year may skew conclusions related to net annual source versus sink status. An estimate for the net carbon (C) import or export through the interface over the seasonally stratified Gulf of Maine is made using an area of roughly 10×10^4 km^2 [cf. *Bisagni*, 2003; *Townsend*, 1991]. In this case, the y axis of Figure 6 will span from −1.8 to +1.8 MtC yr^{-1}, net annual estimates across the stations, and time period range from −0.75 to +1.4 MtC yr^{-1}. The multiyear average for the entire area is +0.45 ± 0.3 MtC yr^{-1}.

[32] How do these results compare with neighboring coastal sites and other reported data? While there are no previous studies dedicated to CO_2 flux estimates in the Gulf of Maine, a recent and extensive compilation of coastal ocean data [*Chavez and Takahashi*, 2007] did provide an estimate of NW Atlantic flux of −1 ± 2 mol m^{-2} yr^{-1} for our approximate study latitude, 42°N (see their Figure 15.4). Their value is based on a limited number of cruises over the period of 1979–2004, with only one cruise within the Gulf of Maine and the rest along the shelf break or along Georges Bank. The present study's multiyear and single-year estimates all lie within their ±2 mol m^{-2} yr^{-1} range of uncertainty, but there is an obvious sink versus source discrepancy when compared with our +0.38 mol m^{-2} yr^{-1} multiyear estimate and an absolute difference near 1.4 mol m^{-2} yr^{-1}. Comparing study observations (Table 1 and Figure 5) with shelf regions to the immediate south shows a similar contrast where the Gulf of Maine, despite its large known rate of gross biological productivity, most often acts as a net CO_2 source, whereas sink levels of −0.7 to −1.6 mol m^{-2} yr^{-1} (±0.5) [*DeGrandpre et al.*, 2002; *Boehme et al.*, 1998] and −0.48 (±0.21) mol m^{-2} yr^{-1} [*Jiang et al.*, 2008] are reported for the Middle Atlantic (MAB) and South Atlantic Bight (SAB) regions, respectively. On the basis, in part, of the data from these cited studies, the *Chavez and Takahashi* [2007] compilation indicates that CO_2 flux values transition from C source to sink as one moves from south to north along the U.S. Atlantic coast. However, use of data exclusively from the studies focused on the SAB, MAB, and GoM would seem to indicate a more complex and perhaps reversed picture along the U.S. NW Atlantic shelf. On a global synthesis level, the status of the GoM as a source is also somewhat in contrast with the *Chen and Borges* [2009] compilation of about 60 marginal sea/continental shelf measurement sites where the global norm shows these areas to be a net sink. In yet another contrast, their sampling of marginal seas shows that these sites generally absorb CO_2 from the atmosphere in the autumn and winter, whereas this is a period of efflux in the Gulf of Maine. We next compare the observed GoM seasonal fCO_2 cycle with neighboring SAB and MAB results using an approach similar to recent studies in the North Sea [*Thomas et al.*, 2005].

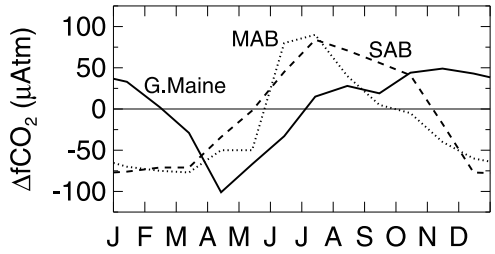

Figure 11. Estimated annual cycle of air-sea ΔfCO_2 for this Gulf of Maine study region (solid), for the Middle Atlantic Bight (dotted), and the South Atlantic Bight (dashed) where the latter two results are derived from *DeGrandpre et al.* [2002] and *Jiang et al.* [2008], respectively.

[33] Figure 11 shows ΔfCO_2 for the three sites, with the SAB and MAB indicating close agreement to one another, particularly when compared to the western GoM. The peak-to-peak ΔfCO_2 seasonal magnitudes at these sites are similar, but there is a marked difference in phase of nearly 100 days, with the annual minimum ΔfCO_2 for SAB and MAB occurring near 1 January (in stronger winter winds), while the WGoM minimum occurs near 1 April when winds are weakening into spring. While a separate study (in preparation, see also *Salisbury et al.* [2009]) will address a finer evaluation of fCO_2 controls, a first-order assessment of these controls is produced in Figure 12 using the approach of *Takahashi et al.* [2002; equations 1–4] as well as its application in the recent coastal C cycle papers of *Schiettecatte et al.* [2006, 2007]. Here the assumption is that one can simulate surface water CO_2 change due to its known isochemical temperature dependence (T) in seawater. The effect of all other processes is termed the biological (BIO) perturbation and can be estimated from the residual gained using the observed and annual mean SST and fCO_2. This BIO term reflects not only biologically mediated CO_2 change, but other perturbing factors including advection, air-sea loss, and riverine input of low DIC and TA waters. Simulated CO_2 time series reflecting temperature and BIO controls are given as

$$fCO_{2T}(t) = fCO_{2m} e^{(0.0423(SST_{obs} - SST_m))} \quad (4)$$

and

$$fCO_{2\,BIO}(t) = fCO_{2obs} e^{(0.0423(SST_m - SST_{obs}))}, \quad (5)$$

where subscripts m and obs refer to annual mean and observed values, respectively. Typical station annual mean values are 10°C and 383 μAtm for SST and fCO_2, respectively. To assess these controlling factors over a 1 year period in regions of seasonal stratification, one can derive a set of residual time series (δfCO_{2BIO}, δfCO_{2T}, and δfCO_{2obs},) by subtraction from the value on a fixed reference day where well-mixed surface layer conditions are observed [*Schiettecatte et al.*, 2006]. For the Gulf of Maine, this day is taken as 15 February, and δfCO_{2T} is given as

$$\delta fCO_{2T}(t) = fCO_{2T}(t) - fCO_{2T}|_{t=\text{day }45}. \quad (6)$$

Results for all three variables and two example years (2005 and 2006) are shown in Figure 12. If the magnitude of δfCO_{2T} exceeds δfCO_{2BIO} (i.e., the ratio is greater than 1), then temperature is the greater control. This is not the case for the western GoM in late March and into summer, where the BIO term is seen to match or exceed T for both years presented (and for the other three not shown). In the latter half of the year, both terms are of similar magnitude. Thus, solubility is typically in competition with other controls throughout the year in the Gulf of Maine. By contrast, *Jiang et al.* [2008] reported a nearly 1:1 correlation between water temperature and fCO_2 dynamics in the SAB (their Figure 10) and conclude that the dominant fCO_2 control is T. Similarly, a temperature-dominated result was seen in the MAB [*DeGrandpre et al.*, 2002]. The competing BIO fCO_2 control within our region is not unexpected [cf. *Salisbury et al.*, 2009] because photosynthetic production is known to greatly exceed that in the SAB and MAB in both magnitude and persistence [*Townsend et al.*, 2006]. But the results do highlight the finding that even though this coastal site exhibits a much larger BIO:T control ratio than the SAB and MAB and one rightly expects a large annual phytoplankton drawdown (sink) of CO_2, the net annual air-sea flux still yields a C export to the atmosphere. Our working explanation for this finding is that, to first order, the annual surface ocean fCO_2 cycle in the GoM follows the observed variation of surface nitrate in the region for the seasonally stratified water column [cf. *Bisagni*, 2003; *Townsend*, 1991]. Put most simply, a strong surface water fCO_2 decline below the atmospheric level occurs each spring-to-summer due to phytoplankton production and riverine impacts, while a nearly corresponding increase above atmospheric levels occurs in middle-to-late autumn and into winter associated with destratification and upward mixing of carbon-replete deeper water. Perturbations attributed to temperature (solubility), air-sea flux, and net community production processes act throughout the year with the net result seen in Figures 5 and 10.

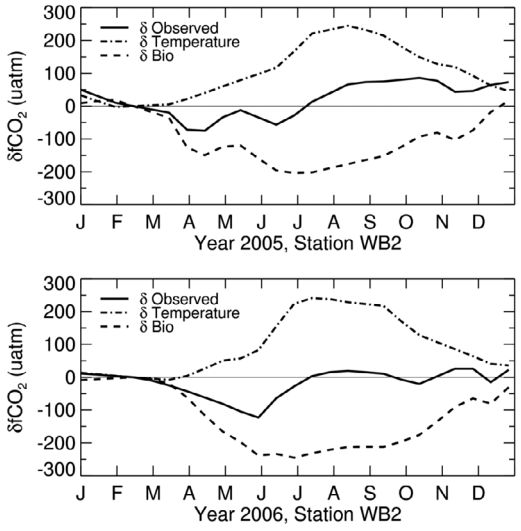

Figure 12. Estimated impact of temperature and all other processes (BIO) on ocean surface layer fCO_2 for two successive years as given by the parameter δfCO_2. Year day 45 (14 February) is chosen as the reference day to null the respective fields.

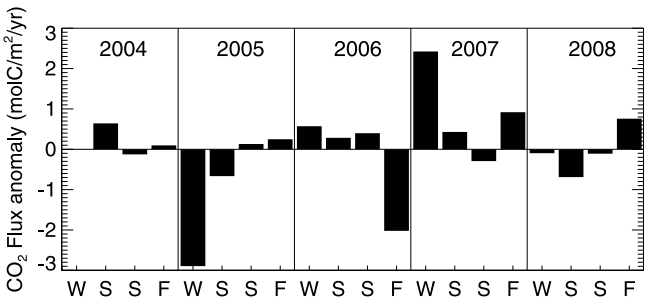

Figure 13. Estimated seasonal air-sea CO_2 flux anomaly at station WB2 over the measurement period 2004–2008. The reference seasonal flux estimates obtained using the 5 year average are +0.2, −3.0, +0.5, +3.6 mol m^{-2} yr^{-1} for the 3 month winter (W), spring (S), summer (S), and fall (F) periods, respectively. All values are given in units of mol m^{-2} yr^{-1}, and winter is taken as January to March.

4.2. Findings Related to Sampling of Temporal CO_2 Variations

[34] We draw several additional conclusions from observations across our region and at time scales of hours to years for both oceanic and atmospheric CO_2.

[35] The daily variability of CO_2 in the atmosphere shown in Figure 3 reveals a complexity that is difficult to quantify using infrequent shipboard measurements; however, this complexity can have a potentially large impact upon the fluxes computed under equation (1). When examining flux modifications due to the recurring diel and seasonal variations in atmospheric CO_2 seen in Figure 3, however, we find limited net impacts (<2%), similar to the comprehensive study of *Padin et al.* [2007]. The variability is attributed to advected continental airflow and, similar to Padin et al. and *Leinweber et al.* [2009], we find the air mass often reflects regional signatures such as daily terrestrial photosynthesis in spring and summer and 2–3 day pollution events (also evident in coincident carbon monoxide data (not shown) collected on Appledore Island) throughout the year. These Gulf of Maine daily CO_2 perturbations generally average out over sufficient time scales, and thus, a least squares harmonic model fit to our data (equation (2)) is adequate for use in monthly and longer-term flux estimates. However, at shorter time scales of hours to weeks, one should avoid a sampling program that collects atmospheric data at a single fixed local time of day, especially in the summer. Such data, without adjustment for unobserved diel variations, will almost certainly bias flux study results conducted over nearly any time scale longer than 3–6 h in this region.

[36] Regarding ocean surface layer fCO_2, the combination of hourly and long-term monthly time series data permit us to resolve several features: the fCO_2 decorrelation time scale is roughly 45 days, M2 tidal dynamics are of second order (see Figure 10), and that episodic variations inside of 30 days can impact monthly derived flux estimates at O(20%–50%) in the spring and fall, with a lesser impact in other times of the year. The effect of such unresolved variations on annual estimates (see Figure 10 and accompanying text) led to significant systematic error of O(0.4 mol m^{-2} yr^{-1}) in our example case. As pointed out in at least three recent studies [cf. *Jiang et al.*, 2008; *Schiettecatte et al.*, 2006, 2007], deriving net annual flux estimates over a coastal region in 1 year and then later revisiting that site in another sampling campaign can lead to differences well beyond 0.4 mol m^{-2} yr^{-1}. These studies attribute differences to a variety of sources, with one being unresolved short-scale temporal variation in ocean fCO_2 as we illustrate in data from April and May 2007 (Figure 10). But our multiyear results in Figure 6 also point to the likelihood that geophysical variability at interannual time scales is also substantial, at least in this region. Both factors corroborate the need to conservatively assign flux estimate uncertainties in coastal data synthesis efforts, particularly for studies having only one year of results (e.g., from four to six cruises), as well as the need to establish long-term monitoring in regions of particular interest. The relative dominance of temporal versus spatial factors observed with respect to air-sea exchange in the Gulf of Maine suggests that a limited network of moorings may serve to monitor this region's air-sea gas flux with relatively high accuracy. This suggestion is tempered by the need to assess spatial and temporal dynamics nearer to the eastern Gulf that is strongly coupled to the Bay of Fundy and M2 tidal mixing and similarly for the large and shallow Georges Bank region to the south.

[37] As a final point, we return to the topic of interannual variability. Figures 5 and 6 suggest substantial annual flux anomalies for years 2005 and 2007. By inspection of Figure 5 and use of equation (1), it is apparent that the deviations are largely due to perturbations in fCO_2 and not seasonal gas transfer (wind) changes in those years. Figure 13 shows the seasonal flux anomaly (units of mol m^{-2} yr^{-1}) computed over the 2004–2008 period at WB2. While this paper has shown that greatest observed short-scale variation in ocean fCO_2 occurs here in the spring and fall, Figure 13 indicates that the largest observed seasonal flux anomalies, especially in 2005 and 2007, occurred in winter (January to March) and this is the season dominating the interannual differences in our data collection to date. Future work will thus include a focus on this winter period and its possible preconditioning by interannual variations in fall destratification, early winter storm mixing, heat flux events, and biochemistry below the mixed layer.

5. Summary

[38] Multiyear shipboard fCO_2 data and air-sea flux estimates in the Gulf of Maine for the period 2004–2008 indicate that this marginal sea coastal region acted as a net source of CO_2 to the atmosphere of $+0.38 \pm 0.26$ mol m^{-2} yr^{-1}. A strong seasonal cycle in both ΔfCO_2 and the air-sea flux is observed, with a large springtime sink offset by a large fall-to-winter efflux. A significant part of this regions' net source status is explained by the coincidence of highest winds and above atmospheric fCO_2 in the winter months. Observed spatial variations were found to be of second order compared to temporal dynamics, and our observations are considered to scale to about 40% of the Gulf of Maine. On average and under this scaling assumption, this region delivered roughly 0.4 MtC (TgC) to the atmosphere per year. Interannual variability in the flux is observed at a level of 0.5 mol m^{-2} yr^{-1}, with 2005 being the only year found to be a sink (−0.1 mol m^{-2} yr^{-1}). Bihourly MAPCO2 time series measurements are used to show that [*ca*] monthly cruise data can under sample fCO_2 dynamics in this system. The ship versus buoy data

comparison allows an identification and estimation of systematic error that is not unexpected, but often unresolved in similar flux field studies. A cursory assessment of controls on the seasonal fCO_2 cycle shows that factors other than temperature dominate ocean solubility in the spring and through the period of the seasonally stratified mixed layer, in agreement with *Salisbury et al.* [2009]. This contrasts with the thermally dominated SAB and MAB regions to the south. Combined ship and buoy measurements continue into 2010 and are being used in several process control studies aimed at empirical and numerical prediction to better understand inorganic carbon dynamics within this system at differing time scales. Moreover, the air-sea flux for adjoining Bay of Fundy and Georges Bank regions will likely act quite differently than for the seasonally stratified waters surrounding our site. Thus, an accounting for the full Gulf of Maine will require an expanded sampling and modeling effort. A final general conclusion is that the complexity gained with increased resolution and extended time series data suggests both caution in data interpretation with respect to statistical confidence in the observations under study and the potential for improved understanding and definition of C cycling in this region.

[39] **Acknowledgments.** We gratefully acknowledge those who helped collect these data including K. Carpenter, R. Varner, S. Musielewicz, the staff of the Gulf of Maine Ocean Observing System and NOAA's National Data Buoy Center, and the crew of the R/V Gulf Challenger. We also thank the directors who initiated the project, J. Campbell and R. Talbot. This work was funded in part by NOAA grants to UNH for AIRMAP NA05OAR4601080 and NA06OAR4600189, NOAA grants NA05-NOS4731206 and NA160C2740, NASA Earth Science Division grant NNX08AL80G, and NSF grant OCE-0851447. This work is NOAA/PMEL contribution 3595.

References

Bakker, D. C. E., J. Etcheto, J. Boutin, and L. Merlivat (2001), Variability of surface water fCO_2 during seasonal upwelling in the equatorial Atlantic Ocean as observed by a drifting buoy, *J. Geophys. Res.*, *106*(C5), 9241–9253, doi:10.1029/1999JC000275.

Balch, W. M., D. T. Drapeau, B. C. Bowler, E. S. Booth, J. L. Goes, A. Ashe, and J. M. Frye (2004), A multirecord of hydrographic and bio-optical properties in the Gulf of Maine: Part I. Spatial and temporal variability, *Prog. Oceanogr.*, *63*, 57–98.

Balch, W. M., D. T. Drapeau, B. C. Bowler, E. S. Booth, J. L. Goes, L. A. Windecker, A. Ashe, and J. M. Frye (2008), Space-time variability of carbon standing stocks and fixation rates in the Gulf of Maine, along the GNATS transect between Portland, ME, USA and Yarmouth, Nova Scotia, Canada, *J. Plankton Res.*, *30*(2), 119–139.

Bates, N. R. (2001), Interannual variability of oceanic CO_2 and biochemical properties in the western North Atlantic subtropical gyre, *Deep Sea Res. Part II*, *48*, 1507–1528.

Bigelow, H. B. (1927), Physical oceanography of the Gulf of Maine, *Bull. U.S. Bur. Fish.*, *40*, 511–1027.

Bisagni, J. J. (2003), Seasonal variability of nitrate supply and potential new production in the Gulf of Maine and Georges Bank regions, *J. Geophys. Res.*, *108*(C11), 8015, doi:10.1029/2001JC001136.

Boehme, S. E., C. L. Sabine, and C. E. Reimers (1998), CO_2 fluxes from a coastal transect: A time series approach, *Mar. Chem.*, *63*, 49–67.

Brooks, D. A. (1985), Vernal circulation in the Gulf of Maine, *J. Geophys. Res.*, *90*(C3), 4687–4706, doi:10.1029/JC090iC03p04687.

Cai, W.-J., M. Dai, and Y. Wang (2006), Air-sea exchange of carbon dioxide in ocean margins: A province-based synthesis, *Geophys. Res. Lett.*, *33*, L12603, doi:10.1029/2006GL026219.

Chavez, F., and T. Takahashi (2007), Coastal oceans, in *The First State of the Carbon Cycle Report (SOCCR): North American Carbon Budget and Implications for the Global Carbon Cycle*, edited by A. W. King et al., pp. 83–92, NOAA, Silver Spring, Md.

Chen, A. C.-T., and A. V. Borges (2009), Reconciling opposing views on carbon cycling in the coastl ocean: Continental shelves as sinks and near-shore ecosystems as sources of atmospheric CO_2, *Deep Sea Res. Part II*, *56*, 578–590.

DeGrandpre, M. D., G. J. Olbu, C. M. Beatty, and T. R. Hammar (2002), Air-sea CO_2 fluxes on the U.S. Middle Atlantic Bight, *Deep Sea Res. Part II*, *49*(20), 4355–4367.

Dickson, A. G., C. L. Sabine, and J. R. Christian (Eds.) (2007), *Guide to Best Practices for Ocean CO_2 Measurements*, *PICES Spec. Publ. Ser.*, vol. 3, 191 pp., North Pac. Mar. Sci. Organ., Sidney, B. C., Canada.

Doney, S. C., B. Tilbrook, S. Roy, N. Metzl, C. LeQuere, M. Hood, R. A. Feeley, and D. Bakker (2009), Surface-ocean CO_2 variability and vulnerability, *Deep Sea Res. Part II*, *56*, 504–511, doi:10.1016/j.dsr2.2008.12.016.

Fairall, C. W., E. F. Bradley, J. E. Hare, A. A. Grachev, and J. B. Edson (2003), Bulk parameterization of air-sea fluxes: Updates and verification for the COARE algorithm, *J. Clim.*, *16*(4), 571–591.

Friederich, G. E., P. G. Brewer, R. Herlien, and F. P. Chavez (1995), Measurement of sea surface partial pressure of CO_2 from a moored buoy, *Deep Sea Res. Part I*, *42*, 1175–1186.

Friederich, G. E., P. M. Walz, M. G. Burczynski, and F. P. Chavez (2002), Inorganic carbon in the central California upwelling system during the 1997–1999 El Nino–La Nina event, *Prog. Oceanogr.*, *54*, 185–203.

Geyer, W. R., R. P. Signell, D. A. Fong, J. Wang, D. M. Anderson, and B. A. Keafer (2004), The freshwater transport and dynamics of the western Maine coastal current, *Cont. Shelf Res.*, *24*(12), 1339–1357.

Ho, D. T., C. S. Law, M. J. Smith, P. Schlosser, M. Harvey, and P. Hill (2006), Measurements of air-sea gas exchange at high wind speeds in the Southern Ocean: Implications for global parameterizations, *Geophys. Res. Lett.*, *33*, L16611, doi:10.1029/2006GL026817.

Jiang, Li-Q., W.-J. Cai, R. Wanninkhof, Y. Wang, and H. Luger (2008), Air-sea CO_2 fluxes on the U.S. South Atlantic Bight: Spatial and seasonal variability, *J. Geophys. Res.*, *113*, C07019, doi:10.1029/2007JC004366.

Keeling, C. D., H. Brix, and N. Gruber (2004), Seasonal and long-term dynamics of the upper ocean carbon cycle at Station ALOHA near Hawaii, *Global Biogeochem. Cycles*, *18*, GB4006, doi:10.1029/2004GB002227.

Kuss, J., W. Roeder, K.-P. Wlost, and M. D. DeGrandpre (2006), Time-series of surface water CO_2 and oxygen measurements on a platform in the central Arkona Sea (Baltic Sea): Seasonality of uptake and release, *Mar. Chem.*, *101*, 220–232, doi:10.1016/j.marchem.2006.03.004.

Leinweber, A., N. Gruber, H. Frenzel, G. E. Friederich, and F. P. Chavez (2009), Diurnal carbon cycling in the surface ocean and lower atmosphere of Santa Monica Bay, California, *Geophys. Res. Lett.*, *36*, L08601, doi:10.1029/2008GL037018.

Manning, J. P., D. J. McGillicuddy Jr., N. R. Pettigrew, J. H. Churchill, and L. S. Incze (2009), Drifter observations of the Gulf of Maine coastal current, *Cont. Shelf Res.*, *29*, 835–845, doi:10.1016/j.csr.2008.12.008.

McGillis, W. R., et al. (2004), Air-sea CO_2 exchange in the equatorial Pacific, *J. Geophys. Res.*, *109*, C08S02, doi:10.1029/2003JC002256.

McNeil, C. L., B. Ward, W. R. McGillis, M. D. DeGrandpre, and L. Marcinowski (2006), Fluxes of N2, O2, CO_2 in nearshore waters off Martha's Vineyard, *Cont. Shelf. Res.*, *26*(11), 1281–1294.

Nightingale, P. D., G. Malin, C. S. Law, A. J. Watson, P. S. Liss, M. I. Liddicoat, J. Boutin, and R. C. Upstill-Goddard (2000), In situ evaluation of air-sea gas exchange parameterizations using novel conservative and volatile tracers, *Global Biogeochem. Cycles*, *14*(1), 373–387, doi:10.1029/1999GB900091.

Olsen, A., R. Wanninkhof, J. A. Trinanes, and T. Johannessen (2005), The effect of wind speed products and wind speed-gas exchange relationships on interannual variability of the air-sea CO_2 gas transfer velocity, *Tellus B*, *57*, 95–106.

O'Reilly, J. E., and D. A. Busch (1984), Phytoplankton primary production on the northwestern Atlantic shelf, *Rapp. P.-V. Reun. Cons. Int. Explor. Mer*, *183*, 255–268.

Padin, X. A., M. Vasquez-Rodriguez, A. F. Rios, and F. F. Perez (2007), Atmospheric CO_2 measurements and error analysis on seasonal air-sea CO_2 fluxes in the Bay of Biscay, *J. Mar. Syst.*, *66*, 285–296.

Perez, F. F., J. Gago, M. Alvarez, and A. F. Rios (2001), Temporal variability of atmospheric CO_2 of the Spanish Atlantic coast, *Oceanol. Acta*, *24*, 11–18.

Pettigrew, N. R., J. H. Churchill, C. D. Janzen, L. J. Magnum, R. P. Signell, A. C. Thomas, D. W. Townsend, J. P. Wallinga, and H. Xue (2005), The kinematic and hydrographic structure of the Gulf of Maine Coastal Current, *Deep Sea Res. Part II*, *52*, 2369–2391.

Pringle, J. M. (2006), Sources of variability in Gulf of Maine circulation, *Deep Sea Res. Part II*, *53*, 2457–2476.

Riley, G. A. (1957), Phytoplankton of the north central Sargasso Sea, 1950–52, *Limnol. Oceanogr.*, *2*, 252–270.

Salisbury, J. E., D. Vandemark, C. W. Hunt, J. W. Campbell, W. R. McGillis, and W. H. McDowell (2008), Seasonal observations of surface waters in two Gulf of Maine estuary-plume systems: Relationships between watershed attributes, optical measurements and surface pCO_2, *Estuarine Coastal Shelf Sci.*, *77*, 245–252.

Salisbury, J. S., D. Vandemark, C. Hunt, B. Jonsson, A. Mahadevan, and W. R. McGillis (2009), Episodic riverine influence on surface DIC in the coastal Gulf of Maine, *Estuarine Coastal Shelf Sci.*, *82*, 108–118.

Schiettecatte, L.-S., H. Thomas, Y. Bozec, and A. V. Borges (2007), High temporal coverage of carbon dioxide measurements in the Southern Bight of the North Sea, *Mar. Chem.*, *106*, 151–163.

Schiettecatte, L.-S., F. Gazeau, C. van der Zee, N. Brion, and A. V. Borges (2006), Time series of partial pressure of carbon dioxide (2001–2004) and preliminary inorganic carbon budget in the Schedlt plume (Belgian coastal waters), *Geochem. Geophys. Geosyst.*, *7*, Q06009, doi:10.1029/2005GC001161.

Shellito, S. M., J. D. Irish, D. Vandemark, S. Maenner, and C. L. Sabine (2008), Time series measurements of atmospheric and oceanic CO_2 and O_2 in the western Gulf of Maine, paper presented at OCEANS 2008, Inst. of Electr. and Electr. Eng., Quebec City, Que., Canada, 15–18 Sept.

Takahashi, T., et al. (2002), Global sea-air CO_2 flux based on climatological surface ocean pCO_2 and seasonal biological and temperature effects, *Deep Sea Res. Part II*, *49*, 1601–1622.

Takahashi, T., et al. (2009), Climatological mean and decadal change in surface ocean pCO_2, and net sea-air CO_2 flux over the global ocean, *Deep Sea Res. Part II*, *56*, 554–577, doi:10.1016/j.dsr2.2008.12.009.

Thomas, H., Y. Bozec, K. Elkalay, H. J. W. debar, A. V. Borges, and L.-S. Schiettecatte (2005), Controls of the surface water partial pressure of CO_2 in the North Sea, *Biogeosciences*, *2*, 232–334.

Townsend, D. W. (1991), Influences of oceanographic processes on the biological productivity of the Gulf of Maine, *Rev. Aquat. Sci.*, *5*, 211–230.

Townsend, D. W., A. C. Thomas, L. M. Mayer, M. Thomas, and J. Quinlan (2006), Oceanography of the Northwest Atlantic continental shelf, in *The Sea*, vol. 14, edited by A. R. Robinson and K. H. Brink, pp. 119–168, Harvard Univ. Press, Cambridge, Mass.

Wanninkhof, R. (1992), Relationship between gas exchange and wind speed over the ocean, *J. Geophys. Res.*, *97*(C5), 7373–7381, doi:10.1029/92JC00188.

Wanninkhof, R., and W. R. McGillis (1999), A cubic relationship between air-sea CO_2 exchange and wind speed, *Geophys. Res. Lett.*, *26*(13), 1889–1892, doi:10.1029/1999GL900363.

Wanninkhof, R., and K. Thoning (1993), Measurement of fugacity of CO_2 in surface water using continuous and discrete sampling methods, *Mar. Chem.*, *44*, 189–204.

Wanninkhof, R., W. E. Asher, D. T. Ho, C. Sweeney, and W. R. McGillis (2009), Advances in quantifying air-sea gas exchange and environmental forcing, *Annu. Rev. Mar. Sci.*, *1*, 213–244, doi:10.1146/annurev.marine.010908.163742.

Weiss, R. F. (1974), Carbon dioxide in water and seawater: the solubility of a non-ideal gas, *Mar. Chem.*, *2*, 203–215, doi:10.1016/0304-4203(74)90015-2.

World Meteorological Organization (1966), Climatic change, 80 pp., *Tech. Note 79/WMO195/TP-100*, Geneva, Switzerland.

Zhou, Y., R. K. Varner, R. S. Russo, O. W. Wingenter, K. B. Haase, R. W. Talbot, and B. C. Sive (2005), Coastal water source of short-lived halocarbons in New England, *J. Geophys. Res.*, *110*, D21302, doi:10.1029/2004JD005603.

C. W. Hunt, J. E. Salisbury, S. M. Shellito, and D. Vandemark, OPAL, EOS, University of New Hampshire, 142 Morse Hall, 8 College Rd., Durham, NH 03824, USA. (doug.vandemark@unh.edu)

J. D. Irish, Ocean Engineering Program, University of New Hampshire, Jere A. Chase Ocean Engineering Building, 24 Colovos Rd., Durham, NH 03824, USA.

S. M. Maenner and C. L. Sabine, NOAA Pacific Marine Environmental Laboratory, 7600 Sand Point Way, NE, Seattle, WA 98115, USA.

W. R. McGillis, Lamont Doherty Earth Observatory at Columbia University, Palisades, NY 10964, USA.